Oncology
and Radiotherapy ©
Vol.14 Iss.5:007-011 • RESEARCH ARTICLE

Delineation of brain tumours for radiotherapy patients using image segmentation techniques

Yousif Abdallah

Department of Radiological Science and Medical Imaging, College of Applied Medical Science, Majmaah University, Majmaah, 11952, Saudi Arabia

SUMMARY

Background: Precise radiation segmentation of brain tumours is essential for the definition of Gross Tumour Volumes (GTVs). For sensitive GTV detection, the most comprehensive data may be provided by MRI images. This study was conducted to delineate malignant brain tumours in radiotherapy patients using image segmentation techniques. Materials and Methods: MRI images of 10 patients with astrocytoma were used in this study. A new method of watershed-based segmentation techniques was used to segment the GTVs (region of interest, ROI) in T1-and T2-weighted MRI images. These techniques were used to delineate the GTVs morphologically and accurately and were compared with manually delineated GTVs. To analyse the segmentation technique quantitatively, the Dice similarity coefficient, sensitivity and segmentation specificity were calculated. The images were processed with the MATLAB image processing toolbox. In MRI images, brain tumours can be easily detected if the objects have a sufficient contrast background. Results: The experimental study and the new method achieved quality segmentation, Dice similarity coefficient, sensitivity and specificity values of 0.92 ± 0.09, 0.86 ± 0.03, 0.94 ± 0.06 and 0.90 ± 0.09, respectively, were achieved. For GTV volume segmentation, image detection and filter morphology were conducted by reading the image, completing brain detection, image dilation, image filling, edge removal, and brain smoothing. This study led to an alternative way of showing an object in a divided brain. This method can help remove unwanted background information and improve diagnosis via brain MRI. Conclusion: The new watershed segmentation method allows the semiautomatic segmentation of GTVs. Anatomical and functional MRI images can create a new way to identify radiation therapy goals and methods.

Key words: delineation, brain, MATLAB, radiotherapy, image processing

Address for correspondence:

Yousif Abdallah, Department of Radiological Science and Medical Imaging, College of Applied Medical Science, Majmaah University, Majmaah, 11952, Saudi Arabia, email: y.yousif@mu.edu.sa

Word count: 3222 **Tables:** 00 **Figures:** 09 **References:** 19

Received: - 28 August, 2020

Accepted: - 19 September, 2020

Published: - 28 September, 2020

INTRODUCTION

There are two main tumour types: cancer (malignant) tumours and benign (noncancerous) tumours [1, 2]. Cancer tumours can be classified into primary tumours originating in the brain and secondary tumours more widely distributed beyond the brain called brain metastases. Brain tumours can occur when an abnormal cell is formed. Exposure and exposure to vinyl chloride, ionizing radiation, and hereditary syndromes such as neurofibromatosis, tuberous sclerosis, and Hippel-Lindau disease are rare risk factors [3]. Meningioma was not shown to be a major concern in cell phone exposure studies. A combination of surgery X-rays and chemotherapy may be required. Seizures may require anticonvulsant treatment.

The human brain is a highly specialized organ allowing people to adapt, resist, and act as a control centre for all aspects of the human body. A person's brain helps express sentences, act and communicate feelings and thoughts. There are two types of brain tissue: Gray Matter (GM) and White Matter (WM). Gray matter includes neuronal and glial cells, also known as neuroglia and glia, respectively, which control the centre of the brain and bases, the centre of the white matter's gray matter and includes the caudate, putamen, pallid and claustrum. White matter fibres consist of several axons linking the cortex to other brain regions. The left and right hemispheres of the brain are linked with a thick band of white matter fibres called the corpus callosum [4]. Cerebrospinal Fluid (CSF) also includes cholesterol, salts, proteins, and white blood cells. Blood circulates through the brain and spinal cord to prevent damage. The brain and spinal cord also contain a tissue called meninges. It is the brain's core. Intelligence is the brain's bulk. It is associated with emotions, movement, and consciousness sensations. It has two halves: right and left. Everyone can control the body's face. Moreover, the four lobes of each hemisphere are the frontal, parietal, and occipital lobes. The cerebellum is the second largest part of the brain. This part controls functions of body movement such as walking, balance, posture, and muscle coordination. It is located behind the brain and is attached to the brain stem. The outer gray matter and inner white matter layers are very thin. The spinal cord is also called spine; it is the extension of the brain. The brainstem controls the vital functions of the human body, such as motor, sensory, cardiac, and respiratory functions. It includes the midbrain, pons, and medulla oblongata [4, 5].

Since the mechanism that regulates normal cells regulates brain cell development, under certain conditions, calls can

grow and multiply uncontrolled. An unregulated brain tissue mass is a brain tumour, which affects normal brain function, increasing brain tension. Some brain tissues move, push the skull, or damage other healthy brain tissues by increasing brain pressure [3]. Scientists defined brain tumours by type, location, and benign/malignant. This includes the source and other (primary) factors [6-11]. The WHO has identified 120 types of brain tumours. It focuses on aggressive, less cell-based behaviour. Most tumour types range from grade I to IV. This scale shows increased tumour grading structure due to variation [3]. Brain-borne tumours are key brain tumours and may be benign and do not spread. Less aggressive tumours also increase pain and swelling. Tumours that are more aggressive can grow and spread faster to other tissues. Everyone's diet, radiation exposure, and biological characteristics differ. Secondary brain tumours originate in other body regions. Melanoma, prostate cancer, other sarcomas, and testicular and germ cell tumours are the most common causes of secondary brain tumours. Cancer tumours may metastasize and spread to the brain.

MRI is not fully automated nor incorporates high-speed cortical segmentation [12]. Radiofrequency (RF) inhomogeneity in data collection results in a shading effect [13], also known as a bias field. Part volume effect means that more than one type of tissue or class occupies one pixel or voxel in this effect type. The segmentation of MRI output usually involves time-consuming procedures and is used by physicians. The automation process for segmenting MRI outputs is difficult because tumour tissue images are gray and often look like normal tissues.

Functional brain imaging can be defined more stringently. This technique is widely used and includes many techniques that define changes in physiology that accompany brain activity. Different techniques could change. Unlike many *in-vitro* methods used to define brain function, *in-vivo* techniques are usually not about behaviour but about the activities of large neuronal populations. It is, however, very informative, as individual neurons do not work separately but work in large aggregates (e.g., vertical neuron integration in columns of the primary sensory cortex). Despite the small dimensions of the neurons, useful information about brain function in the plane can be obtained with a spatial resolution of only 3 mm or higher. Information is transmitted along brain axons via electric signals. Information is transmitted between neurons by the release of molecular neurotransmitter synapses and their subsequent interactions with specific target neuron receptors. These interactions between neurotransmitters and receptors have led to changes in the current flow of membranes that alter the depolarization potential and the frequency of neuronal membranes. Neuronal and glial metabolism is associated with the release of the neurotransmitters required for energy. The greatest amount of energy is used in or around synapses. As normal production of brain energy ultimately depends on oxidative metabolism, local demand for the supply of oxygen increases with increased synaptic activity. Increased local blood flow comes with activation of the neurons to meet increased metabolic demand.

Images have two main features: contrast and detail. To recognize contrast, the human eye must be at least several percent. Calculated rays and digital X-rays can often be used when processing images to adjust and optimize contrast levels and manipulation, e.g., edge enhancements. Ten line pairs per millimetre cannot be detected by human eyes. Each detail is radiologically or spatially unique. All details are associated with simple radiation, fluoroscopy, CT, MRI, ultrasound, and nuclear reduction. Details recorded with simple rays are ideal for identifying mammography details. Many factors undermine the noise image information. In each mode, techniques used to create or view images can inherently add extra noise. For example, ambient light reduces the visual signal-to-noise ratio. When the overhead lights are on, many retinal photons lack diagnostic information. The signal-to-noise ratio is maximized if the overhead light is weak when the video monitor or view box is installed. Radiologists do not work in the dark because they need light but try to minimize the signal-to-noise ratio.

METHODS AND MATERIALS

Images of 10 patients were used in this retrospective study. One of the difficult image processing techniques is segmenting objects in an image. This issue often involves watershed segmentation. The shift is transformed in the image of 'catchment basins' and 'watershed lines' or 'crest lines' as a very light pixel and dark background. Image segmentation results are good when basic objects and locations are marked or identified. Following the following basic procedure, marker-controlled watershed segmentation is accomplished. First, a segmentation function is computed. This is an image whose dark regions are the objects we are trying to segment. Image segmentation is multipart process. This separation is primarily aimed at facilitating image analysis and interpretation while maintaining quality. This technique also traces the edges of objects. This technique labels the intensity values and features. These pieces represent the entire original image, having the same intensity and similarity. For clinical purposes, the picture segmentation technique is used to create a 3D body contour. Segmentation is used in perception, malignant disease analysis, tissue volume analysis, anatomical and functionality analysis, 3D technology, visualization of virtual reality and analysis, definition and object sensing. Images are divided into types: (1) localized and (ii) globally segmented. Local segmentation works in a subdivision of a single image. Compared to the global type, it has fewer pixels. Global segmentation works as a whole unit. More pixels are required for this technique (Figure 1).

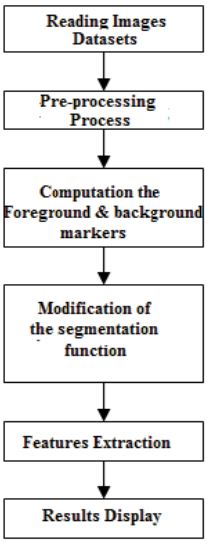

Fig. 1. The brain tumour segmentation steps

Brain tumour segmentation steps using MATLAB

The segmentation depends on the threshold for the grayscale image [4]. Many other radiological techniques also reconstruct images, including Otsu's method and the K-means clustering algorithm [5, 6]. The threshold approach allows placing solid items on a dark background. Threshold techniques require intensity and background changes. There are three threshold approaches. These processes include an adaptive, histogram-based global selection threshold. The global threshold for all division techniques is wide. This equation is estimated using (almost) the global binarization process threshold. The intensity and background information can be collected faster in adaptive or fixed threshold scenarios. The region of interest has its own intensity. The disadvantage of this method is that multichannel images are simple and cannot be processed [14, 15].

$$f(x) = \{^{1\ if\ f\ (m,n) \geq \theta}_{0}$$

T1-weighted images were taken with the fast spin-echo sequence. The fast spin-echo sequence took T2-weighted images. A spin-echo sequence also obtained DWI images. DTI images were captured with planar spin-echo sequences, diffusion-sensitivity gradient encryption, and a series of images in 25 directions. All the images are taken with a 1.5 T MRI scanner, and the original images were analysed at the workstation. Four resolution and spatial coordinate parameters were varied. Hard skull bone covers the brain tissue, causing a smooth, flat transformation. To correct for differences, the rigid body was recorded in 3D. The image sets T2, ADC, and FA were transformed to same size as the main image set T1C with cubic spline interpolation. MIM 5.2 was used to complete registration with the assisted alignment method, a 6-grade automated image registration tool based on a gray image rather than an Atlas template. The assisted alignment procedure optimized mutual data measurement, resulting in alignment of less than a voxel, partial voxel translation and angular rotation (Figure 2). For manually defined GTV (G) comparisons and semi automatically divided GTV (S) comparisons, the segmentation quality measure Q was used. Q was calculated for each individual [16-19].

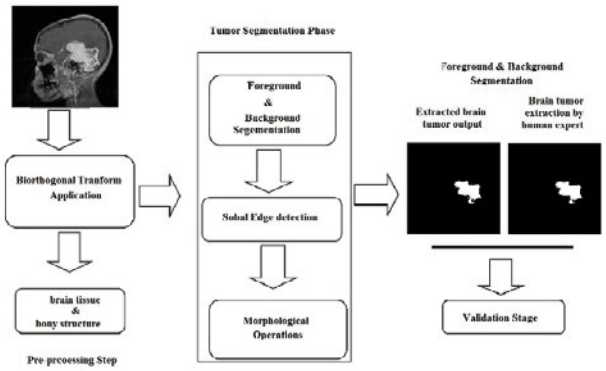

Fig. 2. Brain tumour segmentation steps using MATLAB

RESULTS

This experimental study was conducted to find an accurate brain tumour segmentation method using a parallel computing algorithm. For ten patients with T1 and T2 MRI data, a new potential field segmentation algorithm was used. In total, 200 MRI images were used in this was study. The manually defined fields compared segmented GTVs with the Q, DSC, and other measures. Figure 3 shows the original images before applying watershed segmentation. Figure 4 shows the application of the Sobel edge masks that were used for gradient magnitude computation. Masks, image filters, and a few simple arithmetic methods were used to measure the gradient magnitude. The gradient is high at the object's border, and those of the objects are (mostly) low inside. Figure 5 shows the results of the opening-by-reconstruction algorithm using the opening-close reconstruction filter.

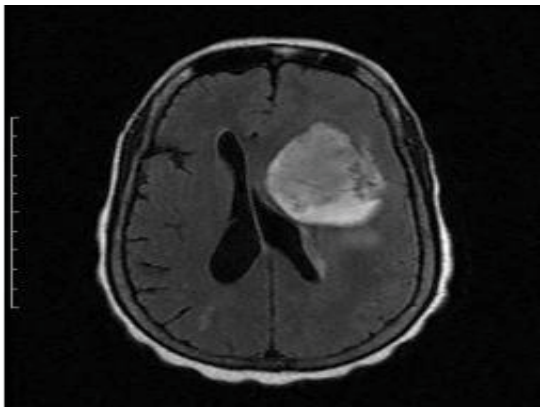

Fig. 3. Original image

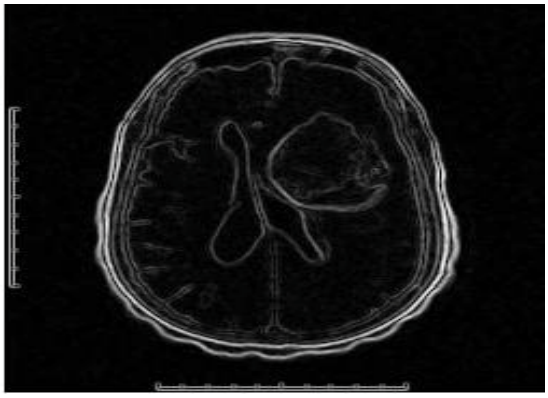

Fig. 4. Gradient magnitude as the segmentation function

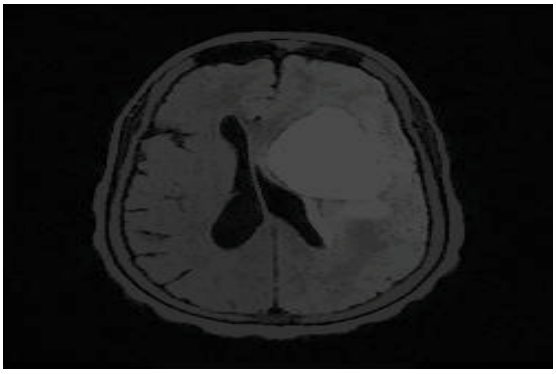

Fig. 5. Opening-by-reconstruction operation

Figure 6 shows image reconstruction results of the registered MRI images and the fusion of the segmented GTV within the original image. Table 1 presents the segmentation quality, Dice similarity coefficient, and sensitivity and specificity evaluations. The segmentation quality values in all the patients ranging from 0.81 to 0.87 are higher or more similar to the average global

FLAIR segmentation potential. The Dice similarity coefficient values range from 0.84 to 0.96. The mean Dice similarity coefficient is 0.92 (± 0.09), and is very consistent across the semiautomatic and manual segmentation methods. The sensitivity and specificity were 0.94 (± 0.06) and 0.90 (± 0.09), respectively, indicating that GTVs are effective in brain tumour segmentation compared to the manually defined ground-truth images (Figures 7-9).

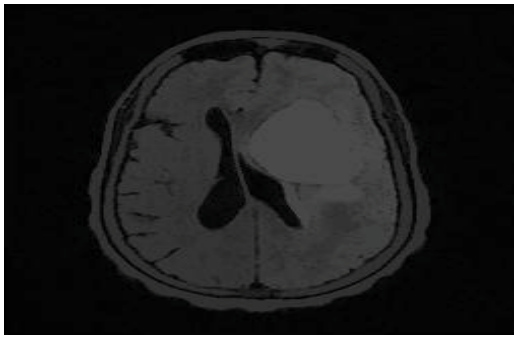

Fig. 6. Opening-closing by reconstruction algorithm

Fig. 7. Regional maxima of opening-closing

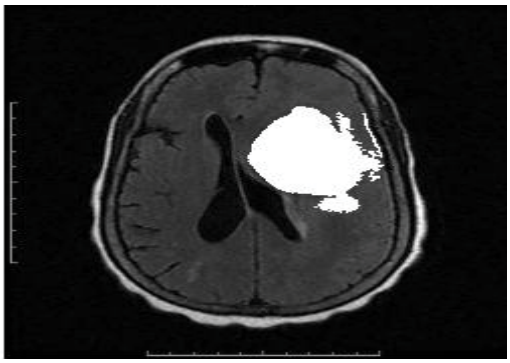

Fig. 8. Regional maxima superimposed on the original image

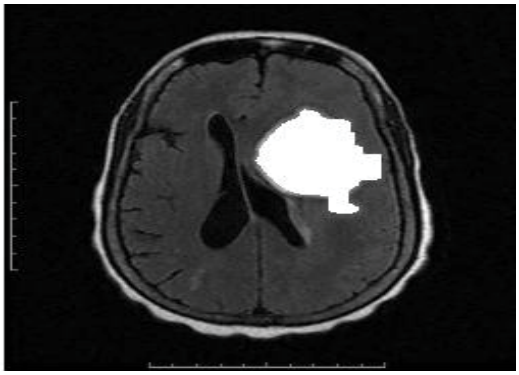

Fig. 9. Modified regional maxima superimposed on the original image

DISCUSSION

An exact method for brain tumour segmentation using a parallel computing algorithm was examined in this experimental study. In addition, an improvement in soft tissue contrast in RIV images is evaluated using a new nonlinear approach for automatic brain tumour extraction. The majority of filters are used in high-or low-frequency images to remove image edges. Filters are usually used to process the images. Photographs are often poor because of various factors. Researcher use pre-processing techniques to remove artifacts such as bleeding, noise and degradation. A number of nonlinear filters have been developed. Although their properties and applications have not been thoroughly studied, they are usually not presented for fourier analysis. This phenomenon led to the use of medium and anisotropic filters by scientists. Algorithms use anisotropic and median filtration methods. GTVs are used in brain tumour radiation therapy to detect anatomical and functional MRI images, and in providing specific information and image features, each image parameter has its advantages. Nevertheless, multipara metric images are difficult to segment with a single approach.

CONCLUSION

This study developed and used a new potential segmentation algorithm applying different post-processing approaches to assess the viability of multipara meter M-RI, including T1-and T2-weighted MRI. Compared with the ground-truth images, the results were satisfactory. In addition to other post-processing approaches, multipara meter image segmentation works well. A series of morphological post processing steps were added to address these deficiencies in the T1-and T2-weighted images. Local PFS has determined the initial FA image seed and fully segmented the growing areas. Compared with existing automatic segmentation methods mainly based on machine training techniques, no training procedures are required. Tuning conditions with fewer parameters improve the efficiency and stability of segmentation. The results from possible new field division processes are satisfactory in terms of the segmentation quality measures, many coefficients and high sensitivity and specificity. To demonstrate the strength of the algorithm, a standard deviation parameter (<0.1) is used. When evaluating low-grade glioma segmentation, the lower 4 values of these five parameters are probably due to a lower image contrast than in the high-grade glioma segmentation task. The multipara metric image synthesis method of this study provided a more exact and comprehensive reference for the definition of GTV in radiation therapy than previous methods. When a single parametric image cannot be shown for the tumour; multipara meter image fusion is a useful tool for precisely defining the boundary for radiation therapy of GTV during disease treatment and to protect healthy tissue. Images of glioma patients have also been tested with a possible field segmentation algorithm and other sites or tumours have not studied. Moreover, there was no distinction between the possible field segmentation results between neoplasms and edema. Furthermore, the development of tissue identification for neoplasms may be further explored.

ACKNOWLEDGEMENTS

The author is thankful to the Deanship of Scientific Research, at Majmaah University for funding this research.

CONFLICT OF INTEREST

No potential conflict of interest relevant to this article was reported.

REFERENCES

1. Ferlay J, Shin HR, Bray F, Forman D, Mathers C, et al. Estimates of worldwide burden of cancer in 2008: GLOBOCAN 2008. Int J Cancer. 2010;127:2893-2917.
2. Louis DN, Ohgaki H, Wiestler OD, Cavenee WK. The 2016 world health organization classification of tumours of the central nervous system: a summary. Acta Neuropathol. 2016;131:803-820.
3. Noback CR, Strominger NL, Demarest RJ, Ruggiero DA. The human nervous system: structure and function. Humana Press. 2005.
4. Buckner JC , Brown PD, O'Neill BP, Meyer FB, Wetmore CJ, et al. Central nervous system tumours. Mayo Clin Proc. 2007;82:1271-1286.
5. Gold LS, Klein G, Carr L, Kesseler L, Sullivan SD. The emergence of diagnostic imaging technologies in breast cancer: discovery, regulatory approval, reimbursement, and adoption in clinical guidelines. Cancer Imaging. 2012;12:13-24.
6. Rodriguez AO. Principles of magnetic resonance Imaging. Revista Mexicana de Fisica. 2004;50:272-286.
7. Novelline RA, Squire LF. Squire's fundamentals of radiology. Harvard Univ Press. 2004.
8. MRI at Glance, Catherine Westbrook. Blackwell Science Publishing. 2002.
9. Prima S, Ayache N, Barrick T, Roberts N. Maximum likelihood estimation of the bias field in MR brain images: investigating different modeling's of the imaging process. Process Med Image Comput and Computer-Assisted Intervention. 2001;2208:811-819.
10. Li X, Li L, Lu H, Chen D, Liang Z. Inhomogeneity correction for magnetic resonance images with fuzzy C-mean algorithm, Proceed of SPIE. 2003;5032:995-1005.
11. Ruan S, Jaggi C, Xue J, Fadili J, Bloyet D. Brain Tissue Classification of Magnetic Resonance Images Using Partial Volume Modeling. IEEE Transactions on Med Imag. 2000;19:1179-1187.
12. Haralick RM, Shapiro LG. SURVEY: image segmentation techniques. Comput Vision Graphics Image Processing. 1985;29:100-132.
13. Sonka M, Hlavac V, Boyle R. Image processing, analysis, and machine vision. Brooks / Cole Publishing Company. 1998.
14. Zucker SW. Region growing: Childhood and adolescence. Comput Graphics Image Process. 1976; 5:382-399.
15. LJ, Hurter D, Naude M, Kritzinger HG, Acho S. A short overview of MRI artifacts. SA J Radiol. 2004;8:13-17.
16. Rastgarpour M, Shanbehzadeh J. Application of AI techniques in medical image segmentation and novel categorization of available methods and tools. Proceedings of the International Multi Conference of Engineers and Computer Scientists. 2011.
17. Kang WX, Yang Q, Liang R. The comparative research on image segmentation algorithms. Intern J All Res Edu Sci Methods. 2009;4:703-707.
18. L. Aurdal, Image Segmentation beyond thresholding. Norsk Regnes central. 2006. Marian W. An automated modified region growing technique for prostate segmentation in trans rectal ultrasound images. Depart Elect Comput Engineer. 2008.